

Original Article

Effects of human induced pluripotent stem cell-derived intestinal organoids on colitis-model mice



Anna Nakanishi^a, Satoshi Toyama^{a,1}, Daichi Onozato^{a,2}, Chihiro Watanabe^b,
Tadahiro Hashita^{a,b,*}, Takahiro Iwao^{a,b}, Tamihide Matsunaga^{a,b}

^a Department of Clinical Pharmacy, Graduate School of Pharmaceutical Sciences, Nagoya City University, 3-1 Tanabe-dori, Mizuho-ku, Nagoya 467-8603, Japan

^b Educational Research Center for Clinical Pharmacy, Faculty of Pharmaceutical Sciences, Nagoya City University, 3-1 Tanabe-dori, Mizuho-ku, Nagoya 467-8603, Japan

ARTICLE INFO

Article history:

Received 14 April 2022

Received in revised form

20 July 2022

Accepted 9 August 2022

Keywords:

Inflammatory bowel disease

Ulcerative colitis

Human induced pluripotent stem cell

Intestinal organoid

Suspension culture

Cell therapy

ABSTRACT

Introduction: Ulcerative colitis (UC) is an inflammatory bowel disease characterized by repeated remissions and relapses. Immunosuppressive drugs have facilitated the induction and maintenance of remission in many patients with UC. However, immunosuppressive drugs cannot directly repair impaired intestinal mucosa and are insufficient for preventing relapse. Therefore, new treatment approaches to repair the damaged epithelium in UC have been attempted through the transplantation of intestinal organoids, which can be differentiated into mucosa by embedding in Matrigel, generated from patient-derived intestinal stem cells. The method, however, poses the challenge of yielding sufficient cells for UC therapy, and patient-derived cells might already have acquired pathological changes. In contrast, human induced pluripotent stem (iPS) cells generated from healthy individuals are infinitely proliferated and can be differentiated into target cells. Recently developed human iPS cell-derived intestinal organoids (HIOs) aim to generate organoids that closely resemble the adult intestine. However, no study till date has reported HIOs injected into *in vivo* inflammatory models, and it remains unclear whether HIOs with cells that closely resemble the adult intestine or with intestinal stem cells retain the better ability to repair tissue in colitis.

Methods: We generated two types of HIOs via suspension culture with and without small-molecule compounds: HIOs that include predominantly more intestinal stem cells [HIO (A)] and those that include predominantly more intestinal epithelial and secretory cells [HIO (B)]. We examined whether the generated HIOs engrafted *in vivo* and compared their ability to accelerate recovery of the damaged tissue.

Results: Findings showed that the HIOs expressed intestinal-specific markers such as caudal-type homeobox 2 (CDX2) and villin, and HIOs engrafted under the kidney capsules of mice. We then injected HIOs into colitis-model mice and found that the weight and clinical score of the mice injected with HIO (A) recovered earlier than that of the mice in the sham group. Further, the production of mucus and the expression of cell proliferation markers and tight junction proteins in the colon tissues of the HIO (A) group were restored to levels similar to those observed in healthy mice. However, neither HIO (A) nor HIO (B) could be engrafted into the colon.

Abbreviations: UC, ulcerative colitis; iPS, induced pluripotent stem; HLA, human leukocyte antigen; HIO, human induced pluripotent stem cell-derived intestinal organoid; SCID-Beige, CB17.Cg-Prkdc^{scid} Lyst^{bg-j}/CrJ; NSG, NOD.Cg-Prkdc^{scid}Il2rg^{tm1Wjl}/Szj; Y-27632, (+)-(R)-trans-4-(1-amino-ethyl)-N-(4-pyridyl) cyclohexanecarboxamide dihydrochloride; A-83-01, 3-(6-methyl-2-pyridinyl)-N-phenyl-4-(4-quinolonyl)-1H-pyrazole-1-carbothioamide; PD98059, 2-(2-amino-3-methoxyphenyl)4-H-1-benzopyran-4-one; 5-aza, 5-aza-2'-deoxycytidine; DAPT, N-[(3,5-difluorophenyl)acetyl]-L-alanyl-2-phenyl-1,1-dimethyl-ethyl ester-glycine; DSS, dextran sodium sulfate; qPCR, quantitative polymerase chain reaction; HPRT, hypoxanthine phosphoribosyltransferase; PBS, phosphate-buffered saline; FBS, fetal bovine serum; DAPI, 4',6-diamidino-2-phenylindole; CDX2, caudal-type homeobox 2; VIL1, villin 1; MUC2, mucin 2; CHGA, chromogranin A; LGR5, leucine-rich repeat-containing G-protein-coupled receptor 5; OLFM4, olfactomedin 4; α -SMA, α -smooth muscle actin.

* Corresponding author. Department of Clinical Pharmacy, Graduate School of Pharmaceutical Sciences, Nagoya City University, 3-1 Tanabe-dori, Mizuho-ku, Nagoya 467-8603, Japan Fax: +81-52-836-3792.

E-mail addresses: c132540@yahoo.co.jp (A. Nakanishi), xmxtq193@yahoo.co.jp (S. Toyama), zatto0515@gmail.com (D. Onozato), yanchiiwatanabe@gmail.com (C. Watanabe), thashita@phar.nagoya-cu.ac.jp (T. Hashita), tiwao@phar.nagoya-cu.ac.jp (T. Iwao), tmatsu@phar.nagoya-cu.ac.jp (T. Matsunaga).

Peer review under responsibility of the Japanese Society for Regenerative Medicine.

¹ Satoshi Toyama: Pfizer Japan Inc., 3-22-7 Yoyogi, Shibuya-ku, Tokyo 151-8589, Japan.

² Daichi Onozato: Eisai Co. Ltd, 4-6-10 Koishikawa, Bunkyo-ku, Tokyo 112-8088, Japan.

<https://doi.org/10.1016/j.reth.2022.08.004>

2352-3204/© 2022, The Japanese Society for Regenerative Medicine. Production and hosting by Elsevier B.V. This is an open access article under the CC BY-NC-ND license (<http://creativecommons.org/licenses/by-nc-nd/4.0/>).

Conclusions: Effective cell therapy should directly repair tissue by engraftment at the site of injury. However, the difference in organoid property impacting the rate of tissue repair in transplantation without engraftment observed in the current study should be considered a critical consideration in the development of regenerative medicine using iPS-derived organoids.

© 2022, The Japanese Society for Regenerative Medicine. Production and hosting by Elsevier B.V. This is an open access article under the CC BY-NC-ND license (<http://creativecommons.org/licenses/by-nc-nd/4.0/>).

1. Introduction

Ulcerative colitis (UC) is a highly prevalent inflammatory bowel disease. Treatment aims to keep the disease in remission for as long as possible, and therapy has improved by targeting the regulation of immune response [1]. Consequently, biological drugs such as anti-tumor necrosis factor- α (TNF- α) antibodies facilitate the induction and maintenance of remission in many patients with UC [2,3]. However, relapse may still take place despite treatment with biological drugs because these drugs are unable to directly repair inflammation-mediated damage in the intestinal mucosa [4–6]. Therefore, repair of the damaged intestinal mucosa while reducing inflammation is important to prevent relapse. The mucosal epithelium works as a barrier against bacterial flora in the lumen of the gastrointestinal tract and as a regulator of immune response via submucosal immune cells, therefore playing an important role in maintaining the body's internal and external harmony [7]. Recent studies have suggested that the disruption of epithelial cell function is a factor in UC pathogenesis [8], and several studies have shown that the risk of relapse can be reduced by not only improving clinical symptoms but also structurally and functionally restoring the mucosal epithelium [6,9].

Many treatments have adopted cell therapy, such as the injection of mesenchymal and intestinal stem cells, as a new method to achieve mucosal recovery. Mesenchymal stem cells are known for their ability to promote the repair of damaged mesenchymal tissues and regulate immunity [10,11]. Therefore, mesenchymal stem cell injection can be expected to repair mesenchymal tissues under intestinal epithelial tissues and help regenerate intestinal epithelial tissues in UC. Meanwhile, intestinal stem cell injection can directly reconstruct ulcers in the intestinal mucosa [12], while Sugimoto et al. reported that injecting human colonic organoids in a mouse with colitis could repair its injured mucosa [13]. Therefore, intestinal organoid injection is an expected treatment for UC. Intestinal organoids are three-dimensional structures containing multiple types of cells that constitute intestinal tissue. Recently, the technique of producing intestinal organoids by embedding human biopsy-derived crypts in Matrigel has allowed the culture and proliferation of intestinal epithelial stem cells *in vitro* [14,15]. However, the embedding method is not appropriate to ensure cell sources for therapy because of the limited area available for culture and the difficulty in obtaining enough cells. Nevertheless, suspension culture can be easily scaled up by simply increasing the amount of medium, a culture technique that must be applied to cell therapy, which is essential to reserve cell count.

Although using patient-derived cells is preferable for the prevention of immune rejection in therapy, patient-derived cells may lead to poor therapeutic efficacy or recurrence. In addition, obtaining sufficient cell quantities from patients for therapy is extremely time-consuming and costly. Thus, healthy human induced pluripotent stem (iPS) cells have gained attention as a new cell resource. Human iPS cells can easily meet cell quantity requirements and can be also generated from a few drops of healthy human blood [16]. Furthermore, plans are underway to generate and stock iPS cells from people with homozygous human leukocyte

antigen (HLA) haplotypes, which are less sensitive to immune rejection [17–19]. Meanwhile, issues include whether enough target cells can be differentiated to use human iPS cells for UC therapy. Although studies have reported several methods to induce differentiation of human iPS cells into intestinal organoids [20–22], these methods use embedding, for which obtaining sufficient number of cells for UC therapy is difficult. Additionally, the specific properties of human iPS cell-derived intestinal organoids (HIOs) that are best suited for UC treatment are unknown. Although recent studies of HIO have aimed to develop HIOs that closely resemble adult intestinal cells, recent regenerative medicine research have been focused on tissue repair by intestinal stem cells. To the best of our knowledge, no reports have evaluated the effect of HIOs in *in vivo* inflammatory models.

Therefore, this study aimed to generate two types of HIOs, predominantly including intestinal stem cells or intestinal cells close to the adult intestine, using our established method as an alternative to embedding and to evaluate whether the generated HIOs accelerate the recovery of damaged tissues.

2. Materials and methods

2.1. Animals

All experimental procedures followed the Regulations for Animal Experimentation at Nagoya City University and were reviewed by the university's Institutional Laboratory Animal Care and Use Committee. CB17. Cg-Prkdc^{scid} Lyst^{bg-J}/CrIcrlj (SCID-Beige) mice (male, 7–10 weeks old) and NOD. Cg-Prkdc^{scid}Il2rg^{tm1Wjl}/SzJ (NSG) mice (male, 8–10 weeks old) were purchased from Charles River Laboratories Japan (Kanagawa, Japan) and were housed in a controlled environment with access to water *ad libitum*.

2.2. Human iPS cells

A human iPS cell line (Windy), which was registered in the Japanese Collection of Research Bioresources Cell Bank, was kindly provided by Dr. Akihiro Umezawa from the National Center for Child Health and Development. Established by Umezawa et al., Windy was derived from the embryonic human lung fibroblast cell line MCR-5 [23] by introducing four factors: OCT3/4, SOX2, KLF4, and c-MYC.

2.3. Culture of iPSCs and differentiation into intestinal organoids

HIOs were generated and maintained according to the previously described method [24]. On day 7, the differentiation cells (7.0×10^6 cells) were passaged onto 100 mm EZSPHERE dishes (AGC Techno Glass Inc., Shizuoka, Japan) to generate spheroids and cultured with (+)-(R)-trans-4-(1-amino-ethyl)-N-(4-pyridyl) cyclohexa-necarboxamide dihydrochloride (Y-27632, Focus Biomolecules, Plymouth Meeting, PA) for three days, after which the spheroids were transferred to ultralow attachment plates (Corning, Corning, NY). From days 19–34 of differentiation, 0.5 μ M 3-(6-methyl-2-pyridinyl)-N-phenyl-4-(4-quinolinyl)-1H-pyrazole-1-carbothioamide (A-83-01, AdooQ BIOSCIENCE, Irvine, CA), 20 μ M 2-(2-

amino-3-methoxyphenyl)4-H-1-benzopyran-4-one (PD98059, AdooQ BIOSCIENCE), 5 μM 5-aza-2'-deoxycytidine (5-aza, Chem-Impex International, Inc., Wood Dale, IL), and 5 μM N-[(3,5-difluorophenyl)acetyl]-L-alanyl-2-phenyl-1,1-dimethyl-ethyl ester-glycine (DAPT, Peptide Institute Inc., Osaka, Japan) were added to the HIO (B) group.

2.4. HIO transplantation

HIOs cultured for 34 days were resuspended in media containing purified type I collagen (Cellmatrix® Type I-A, Nitta Gelatin Inc., Osaka, Japan) for 1 h at 4 °C and were transferred into standard Advanced DMEM/F12 medium. Kidney capsules were transplanted as previously reported by Watson et al. [25,26], after which Spongel® (LTL Pharma, Tokyo, Japan) was placed over the opened kidney capsules to prevent HIO leakage. HIOs, classified as those without small-molecule compounds [HIO (A)] and with small-molecule compounds [HIO (B)], were transplanted into six or eight SCID-Beige mice, respectively, and the transplanted HIOs were harvested after eight weeks.

Acute colitis-model mice were constructed by administering a concentration of 2.5% wt/vol dextran sodium sulfate (DSS, MP Biomedicals, Irvine, CA) with a molecular weight of 36,000–50,000 in drinking water daily for 6 days, as described previously [11,27]. On days 8 and 11, HIOs (equivalent to 2 × 10⁶ cells) were injected into the colonic lumen using a thin flexible catheter 4 cm in length and 1.3 mm in diameter. After the injection, the anal verge was glued for 6 h to prevent the immediate excretion of luminal contents. NSG mice were monitored daily for body weight and clinical scoring such as diarrhea or fecal occult blood. Clinical scores were assigned using a modified scoring sheet, as described previously [11,28,29]. Weight loss percentage was calculated and scored as 0 (no loss), -1 (1%–5%), -2 (5%–10%), -3 (10%–15%), -4 (15%–20%), and -5 (above 20%). Fecal occult blood was scored as 0 (no blood), -1 (mild), and -2 (severe). Scores for fecal consistency were 0 (normal), -1 (moist), and -2 (loose or watery). The final clinical score was the sum of the weight, fecal occult blood, and fecal consistency scores with a maximum level of nine. On day 17, the mice were sacrificed and analyzed.

Table 1 PCR primer and probe sequences.

Human		
Gene	Forward primer sequence (5' → 3')	Reverse primer sequence (5' → 3')
ACTA2	CCGACCGAATGCAGAAGGA	ACAGAGTATTTCGGCTCCGAA
CDX2	ACCTGTGCGAGTGGATGC	TCCTTTGCTCTCGGGTCT
CHGA	TCCGACACACTTTCCAAGCC	TTCTGCTGATGTGCCCTCTC
HPRT	CTTTGCTTTCTTGGTCAGG	TCAAGGGCATATCCTACAACA
LGR5	TGCTCTTACCAACTGCATC	CTCAGGCTCACCAGATCCTC
MUC2	AGAAGGCACCGTATATGACGAC	CAGCGTTACAGACACACTGCTC
OLFM4	CAGACACCACCTTTCTG	CCTTCTCATGATGTCAATTTCG
VIL1	AGCCAGATCACTGAGGT	TGGACAGGTGTTCTCCTCTC
VIM	AGGAAATGGCTCGTCACCTTCGTGAATA	GGAGTGTCCGGTGTGAAGAACTAGAGCT
Mouse		
Gene	Forward primer sequence (5' → 3')	Reverse primer sequence (5' → 3')
Hprt	TTGTTGTAGGATATGCCCTTGA	GCGATGTCAATAGGACTCCAG
Il-1β	GACCTGTTCTTGAAGTTGACG	CTCTTGTGATGTGCTGCTG
Il-6	TCCTTAGCCACTCCTTCTGT	AGCCAGAGTCCTCAGAGA
Tnf-α	AGACCCTCACACTCAGATCA	TCTTTGAGATCCATGCCGTTG
Gene	Probe sequence (5' → 3')	
Hprt	56-FAM/AGCCTAAGA/ZEN/TGAGAGTTCAAGTTGACTTTGG/31ABkFQ	
Il-1β	56-FAM/TTCCAAACC/ZEN/TTTGACCTGGGCTGT/31ABkFQ	
Il-6	56-FAM/CCTACCCCA/ZEN/ATTTCCAATGCTCTCT/31ABkFQ	
Tnf-α	56-FAM/CCACGTCGT/ZEN/AGCAAACCACCAAGT/31ABkFQ	

2.5. Realtime quantitative polymerase chain reaction

Total RNA was extracted using Agencourt RNAdvance Tissue Kit (Beckman Coulter Inc., Brea, CA) according to manufacturer's instructions. cDNA was prepared from 500 ng of total RNA. Reverse-transcription reaction was performed using the ReverTra Ace qPCR RT Kit (TOYOBO, Osaka, Japan). Quantitative polymerase chain reaction (qPCR) with the primers and probes presented in Table 1 was conducted using a KAPA SYBR FAST qPCR Kit or KAPA PROBE Fast qPCR Kit (KAPA Biosystems, Wilmington, MA) and LightCycler 96 system (Roche, Basel, Switzerland). The mRNA expression levels were normalized to those of the encoding hypoxanthine phosphoribosyltransferase (HPRT, human) or Hprt (mouse) gene.

2.6. Immunocytochemistry

HIOs were embedded in an optimal cutting temperature (OCT) compound (Sakura Finetech Japan Co., Ltd., Tokyo, Japan) after fixing with 4% paraformaldehyde and then cut into 10 μm sections. Antigen activation was conducted using 1/200 diluted ImmunoSaver (Nissin EM, Tokyo, Japan) at 98 °C for 45 min. The sections were permeabilized with 0.1% Triton X-100 and, after blocking in phosphate-buffered saline (PBS) containing 5% fetal bovine serum (FBS) for 30 min, reacted with the primary antibodies at 4 °C overnight. The sections were then incubated using Alexa Fluor 488- or 568- conjugated secondary antibodies (Thermo Fisher Scientific) at room temperature for 1 h. Nuclei were stained with 4',6-diamidino-2-phenylindole (DAPI, Dojindo, Kumamoto, Japan) at room temperature for 5 min. The sections were then washed with PBS and mounted using SlowFade Diamond Antifade Mountant (Thermo Fisher Scientific), and confocal images were captured and analyzed using a Zeiss LSM510 microscope and AxioVision software (Carl Zeiss, Oberkochen, Germany).

2.7. Histology and immunohistochemistry

The tissue samples were fixed with 4% paraformaldehyde, after which heat-induced epitope retrieval was conducted by boiling the specimens in 1/200 diluted ImmunoSaver at 98 °C for 45 min.

Endogenous peroxidase was then inactivated by treating the specimens with 0.3% H₂O₂ in methanol at room temperature for 30 min. Next, the specimens were permeabilized with 0.1% Triton X-100. After the specimens were treated with Blocking One solution (Nacalai Tesque, Kyoto, Japan) at room temperature for 30 min, they were incubated with primary antibodies at 4 °C overnight. The sections were stained using ImmPRESS IgG-peroxidase kits (Vector Laboratories, Burlingame, CA) and ImmPACT DAB Peroxidase Substrate Kit (Vector Laboratories) according to supplier instructions. After counterstaining with hematoxylin, the specimens were dehydrated and mounted. Alcian blue staining was performed at pH 2.5, and the nuclei were stained with nuclear fast red. Stained images were captured using All-in-One Fluorescence Microscope BZ-X810, and the positive area of acid mucopolysaccharide was calculated using the Hybrid Cell Count System (KEYENCE, Osaka, Japan). Table 2 shows the primary antibodies and their dilutions.

2.8. Statistical analysis

All data were expressed as mean ± SD. For parametric data, Student's *t*-test or one-way analysis of variance with post-hoc Tukey's multiple comparison was used. For nonparametric data, the Kruskal–Wallis test and Dunn's test for multiple post hoc comparison were employed. Statistical analyses were performed using SPSS Statistics version 25.0 (IBM Japan, Tokyo, Japan). The results were considered significant when *p* < 0.05.

3. Results

3.1. Differentiation of intestinal organoids from human iPS cells

To generate a large volume of uniformly sized spheroids efficiently and simply, we conducted a floating culture using Matrigel-suspended medium. Human iPS cell-derived midguts were seeded on EZSPHERE plates. After culture on the plates for 3 days (Fig. 1A), the size of the spheroids was uniform at about 200 μm. The spheroids were transferred to ultralow attachment plates and cultured in Advanced DMEM/F12 with 3% Matrigel suspension (Fig. 1B). We then generated HIOs from the spheroids with or without A-83-01, PD98059, 5-aza, and DAPT (Fig. 1C). In both groups, the mRNA of caudal-type homeobox 2 (*CDX2*), which is the marker of the hindgut, was expressed as well as the adult small intestine. In addition, the mRNA expression levels of intestinal mature cell markers villin 1 (*VIL1*), mucin 2 (*MUC2*), and chromogranin A (*CHGA*) in group B (HIOs with compounds) were significantly higher than those of group A (HIOs without compounds) (Fig. 1D). However, the mRNA expression of leucine-rich repeat-containing G-protein-coupled receptor 5 (*LGR5*), the intestinal stem cell marker, was significantly higher in group A. The mRNA

expression of vimentin, the mesenchymal cell marker, was higher in both HIO groups than that of adult small intestine (Fig. 1D).

The HIOs expressed villin, olfactomedin 4 (*OLFM4*), *LGR5*, *Ki67* (proliferation marker), *CDX2*, E-cadherin (epithelial cell marker), *CHGA*, vimentin, and α-smooth muscle actin (α-SMA) (Fig. 1E). Interestingly, some markers were expressed locally; those of intestinal cells were expressed near the lumen-like structures where the epithelial cell marker E-cadherin was expressed. In particular, HIO (B) showed that villin expression was localized inside the lumen-like structures. In contrast, vimentin was expressed more on the outer side. *MUC2* and lysozyme, a Paneth cell marker, were expressed only in HIO (B) (Supplementary Fig. 1) and not in HIO (A).

3.2. Transplantation of intestinal organoids into mouse kidney

To determine whether the generated HIOs contained intestinal stem cells, we transplanted the HIOs under the kidney capsules of immunodeficient mice. Eight weeks after transplantation, both HIO groups were engrafted into the kidneys of each mouse (Fig. 2A). However, a difference in grafting efficiency was observed between the two groups. The transplanted HIOs were found in three of the four mice in group A but in only two of the eight mice in group B (data not shown). Fluorescence immunostaining results showed the expression of protein markers present in the intestinal cells in both groups (Fig. 2B). Specifically, villin and *OLFM4* expression levels were similar to those of the HIOs before transplantation; villin was expressed in the inner part of the lumen-like structures whereas *OLFM4* was expressed in the outer part (Figs. 1E and 2B). The expression of vimentin, α-SMA, and occludin was also observed. While lysozyme expression was observed only in group A, *MUC2* expression was found only in group B. These results indicated the *in vivo* maintenance of the properties of intestinal stem cells in transplanted HIOs.

3.3. Injection of HIOs into mouse colitis models

To determine whether the HIOs helped repair damaged intestinal mucosa, we injected HIOs into the colons of DSS colitis-model mice (Fig. 3A). On day 5, the body weight and the clinical score of the colitis-model mice recovered significantly faster in group A compared with the sham group (Fig. 3B and C). On day 9 post-injection, the sham group recovered to the same level as the injection groups in weight, clinical score, and colon length (Fig. 3B–D).

To examine whether the barrier function of the intestinal epithelium after inflammation differed depending on the presence of HIO injection and the properties of the injected HIOs, we stained for acidic mucopolysaccharide, *Ki67*, and ZO-1. After nine days of DSS discontinuation, the sham group showed a significantly higher

Table 2
Primary antibodies for immunostaining.

Antibody	Source	Catalog number	Biological source	Dilution
α-Smooth muscle actin	Abcam	ab5694	Rabbit	1:100
Chromogranin A	IMMUNOSTAR	20085	Rabbit	1:500
CDX2	Abcam	Ab76541	Rabbit	1:100
E-Cadherin	BD Transduction Laboratories	610181	Mouse	1:100
Ki67	eBioscience	14–5699	Mouse	1:200
Ki67	BD Biosciences	550609	Mouse	1:50
Lysozyme	BioGenex	AR024-5R	Rabbit	–
MUC2	Santa Cruz	sc-15334	Rabbit	1:200
Occludin	Thermo Fisher Scientific	71–1500	Rabbit	1:100
OLFM4	Abcam	ab85046	Rabbit	1:100
Villin	Santa Cruz	sc58897	Mouse	1:50
Vimentin	Abcam	ab8069	Mouse	1:100
ZO-1	Thermo Fisher Scientific	33–9100	Mouse	1:100

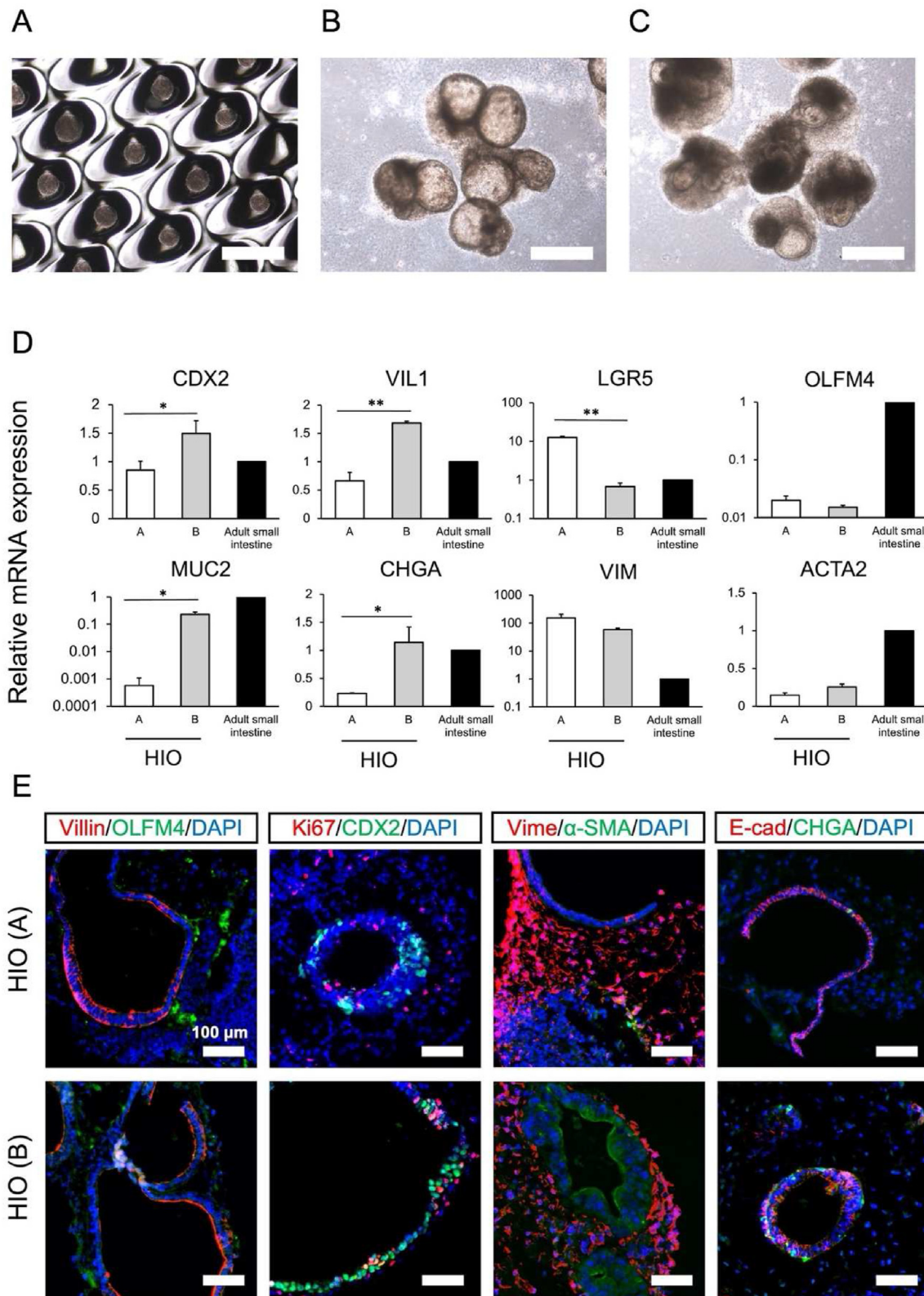


Fig. 1. Morphology and features of human iPS cell-derived intestinal organoids by suspension culture (A) Day 10 of differentiation induction. Spheroids of the differentiation cells cultured for 3 days on EZSPHERE plates (B, C) Day 34 of differentiation induction. Spheroid of (A) transferred to ultralow attachment plates and cultured in Advanced DMEM/F12 containing 3% Matrigel suspension (B) without or (C) with small-molecule compounds at the end of differentiation (day 34) (A–C) Scale bar = 500 μ m (D) Relative mRNA expression of the HIOs cultured without [HIO (A) group] and with [HIO (B) group] small-molecule compounds. SI: total RNA from human adult small intestine samples (five donors), Caudal-type homeobox 2 (*CDX2*), villin 1 (*VIL1*), leucine-rich repeat-containing G-protein-coupled receptor 5 (*LGR5*), olfactomedin 4 (*OLFM4*), mucin 2 (*MUC2*), chromogranin A (*CHGA*), vimentin (*VIM*), and actin alpha 2, smooth muscle (*ACTA2*) are markers of the hindgut, absorptive epithelial cells, intestinal stem cells, goblet cells, enteroendocrine cells, mesenchymal cells, and smooth muscle cells, respectively. The mRNA expression levels of SI were defined as 1. Data were shown as mean \pm SD ($n = 3$). * $p < 0.05$, ** $p < 0.01$ [HIO (A) vs. HIO (B)] (E) Fluorescence immunostaining of HIOs. Ki67 and E-cadherin (E-cad) are markers of cell proliferation and epithelial cells, respectively. Villin, OLFM4, Ki67, CDX2, E-cad, and CHGA were highly expressed in the luminal-like structures, and vimentin (Vime) and α -smooth muscle actin (α -SMA) were expressed outside them. Scale bar = 100 μ m.

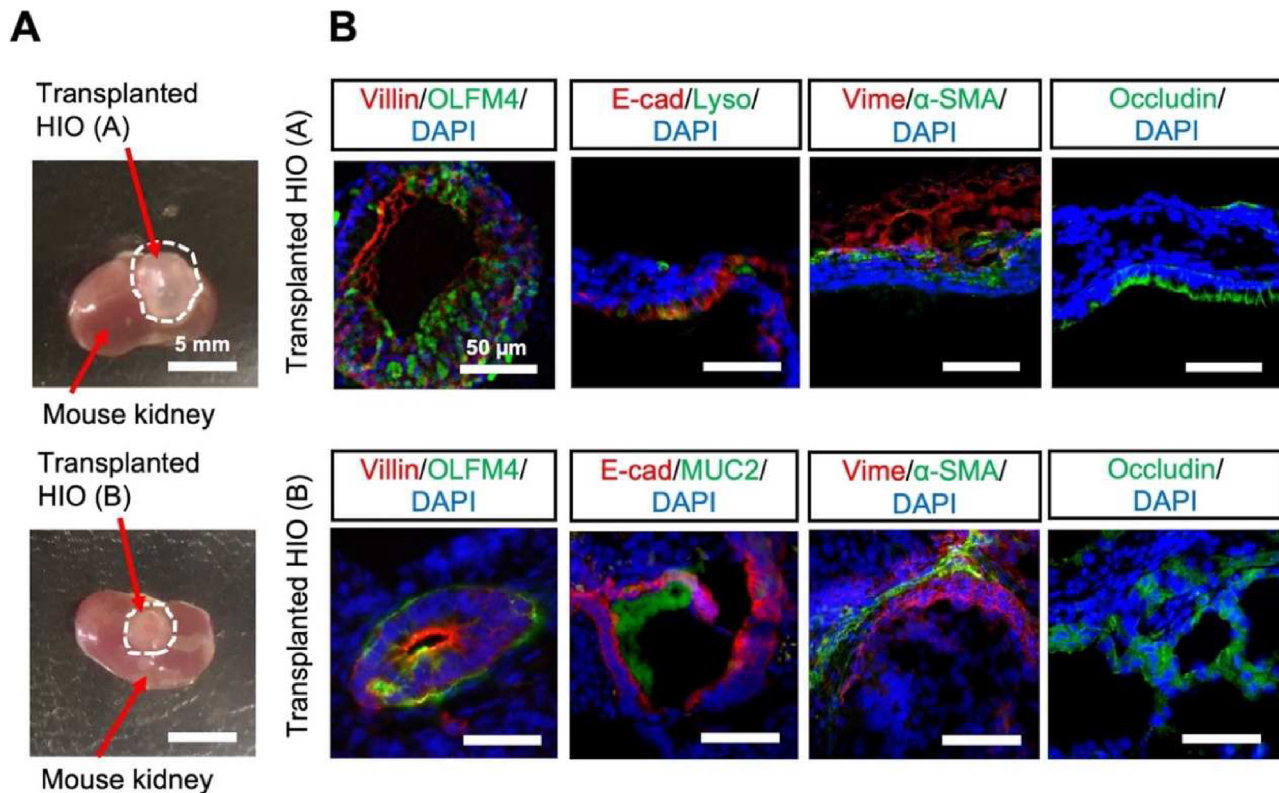


Fig. 2. Engraftment of HIOs transplanted into the kidney capsules of mice (A) HIOs after 8 weeks of transplantation. Scale bar = 5 mm (B) Fluorescence immunostaining of transplanted HIOs. Villin and occludin were expressed inside the lumen-like structures. Lysozyme (Lyso) and occludin are markers of Paneth cells and tight junctions, respectively. Scale bar = 50 μ m.

positive alcian blue staining area than the DSS (–) group, while the positive alcian blue staining area in the HIO (A) injection group was smaller than that of the sham group and comparable to that of the DSS (–) group (Fig. 4A and B). Ki67 was evenly expressed at the bottom of the crypt in the HIO injection groups but was not expressed in some areas in the sham group (Fig. 4C). ZO-1 expression in the upper part of the crypt was weaker in the sham group than in the HIO injection groups (Fig. 4C). These results show that on day 9, the tissues in the sham group were still not completely repaired, suggesting that barrier function status, such as mucus secretion and tight junctions, recovered faster in the HIO (A) injection group than in the sham group.

3.4. Effects of HIO injection on inflammation

To evaluate the extent of inflammatory response against disease, we quantified the expression levels of pro-inflammatory cytokines. The expression levels of *Tnf- α* , *Il-1 β* , and *Il-6* in the HIO injected groups tended to be lower than in the sham group although they were higher than in the DSS (–) group (Fig. 5). Specifically, the *Tnf- α* expression levels in the HIO injection groups were significantly lower than those in the sham group. These results indicate that the sham group was still in an inflamed state on day 9, when their body weight was similar to that of the HIO injection groups, and HIO injection may reduce the activity of pro-inflammatory cytokines.

4. Discussion

This was the first study to report the possible effectiveness of suspension culture-produced HIOs in tissue repair in acute colitis-model mice. Conventional methods generally produce HIOs by

embedding Matrigel or other materials [21,22,30], but these make it difficult to immediately obtain enough organoids for UC therapy. In this study, we used our established suspension culture method to generate HIOs and examined whether these HIOs could accelerate the recovery of damaged tissues. By adopting suspension culture, we expect future experiments to use mass culture via floating culture devices such as bioreactors. Meanwhile, newer differentiation methods such as the exclusion of xenogenic components must be investigated in regenerative medicine, as this study's culture medium contained Matrigel and serum as components of nonhuman origin.

We also produced two HIO types with different levels of expressing intestinal constituent cells in the absence or presence of small-molecule compounds (Fig. 1) and found that those with a higher expression of intestinal stem cell markers showed higher engraftment efficiency under the kidney capsule of mice (Fig. 2) and a greater effect on mucosal repair in acute colitis-model mice (Figs. 3–5). We previously reported the effectiveness of A-83-01/PD98059/5-aza/DAPT in differentiating human iPS cells into intestinal organoids [24]. Adding these compounds during differentiation produced organoids with higher intestinal epithelial cell and secretory cell expression, while the absence of such compounds produced organoids with higher intestinal stem cell expression. However, the lack of reports on the injection of HIOs into colitis-model mice made it unclear which organoid types were more suitable for tissue repair: those with more intestinal differentiated cells such as intestinal epithelial cells and goblet cells or those with more intestinal stem cells. Other studies on injection into colitis-model mice have used biopsy-derived intestinal organoids, which contain both epithelial and stem cells [13,31]. Therefore, we investigated whether there were differences between the two types of HIOs with regard to their engraftment ability under the

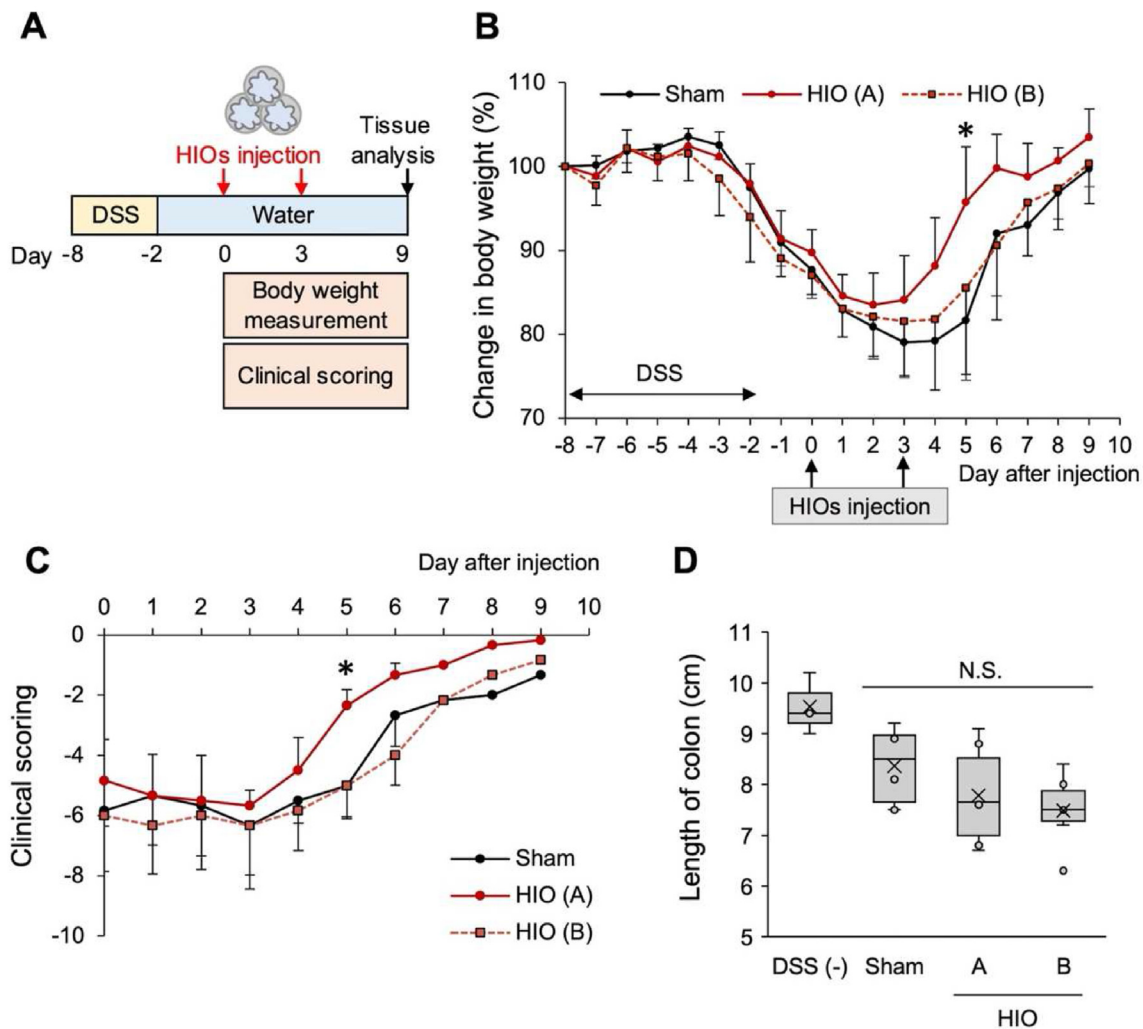


Fig. 3. Improvement of clinical symptoms in colitis-model mice via HIO injection (A) Scheme for constructing colitis-model mice and HIO injection experiments. Acute colitis was induced in mice by drinking water containing 2.5% DSS daily for 6 days. Two injections were performed, with day 0 designated as the day of the first injection. Body weight and clinical scores (weight loss, fecal occult blood, diarrhea) were measured daily, and colon tissues were removed on day 9. NSG mice were randomly assigned to the following groups. DSS (-): untreated control group; sham: DSS; HIO (A): DSS and HIOs without small-molecule compounds; HIO (B): DSS and HIOs with small-molecule compounds (B) Body weight changes of colitis-model mice after injection. The body weight of mice on the first day of DSS administration was defined as 100%. Data were shown as mean \pm SD ($n = 6$). * $p < 0.05$ (vs. sham) (C) Time-dependent change in clinical scores of colitis-model mice after injection. Clinical scores were the sum of weight loss (0 to -5), fecal occult blood (0 to -2), and diarrhea (0 to -2). The minimum possible score was -9. Data were shown as mean \pm SD ($n = 6$). * $p < 0.05$ (vs. sham) (D) Length of colon after 9 days of injection. Data were shown as mean \pm SD [DSS (-): $n = 3$; sham, HIO (A), HIO (B): $n = 6$]. N.S.: not significant.

kidney capsule of mice and their effect on colon tissue injury in acute colitis-model mice.

Before injecting HIOs into colitis-model mice, we transplanted HIOs under the mouse kidney capsules as reported in several studies [25,32] and examined the differences between the two HIO types (Fig. 2). Because the kidney capsule has a high blood flow rate and prevents the transplanted cells from spreading to other locations, the transplanted cells were easy to engraft [33]. In addition, transplanting HIOs *in vivo* makes it possible to confirm whether the intestinal stem cells expressed on the HIOs spontaneously and continuously differentiate into intestinal cells [25]. Eight weeks post-transplantation, both HIO groups engrafted in the mice kidneys (Fig. 2A). Protein expression of intestinal cells was also observed in both groups of HIOs. This shows that even after *in vivo* transplantation in mice, intestinal stem cell properties are preserved. Notably, the two groups showed different HIO sizes and engraftment rates at the time of removal. Approximately 10 HIOs with a diameter of 500 μ m (Fig. 1C) were transplanted for each kidney, and HIOs (A) after 8 weeks of transplantation were

larger and had a higher engraftment rate than HIOs (B) (Fig. 2A). The mRNA expression of intestinal stem cells in HIO (A) was higher than in HIO (B) (Fig. 1D), which might have led to the increase in organoid size and engraftment efficiency. Furthermore, although neither lysozyme nor MUC2 was expressed in HIO (A) before the transplantation, only lysozyme was expressed after the transplantation (Fig. 2B). In contrast, both lysozyme and MUC2 were expressed in HIO (B), in agreement with Onozato et al.'s study (Supplementary Fig. 1) [24]. However, the expression of lysozyme in HIO (B) was lost after the transplantation. These results suggest that the expression of lysozyme was induced in HIO (A) and suppressed in HIO (B) after transplantation. Based on these results, we hypothesize that HIO (A) might be more suitable for injection into colitis-model mice. Meanwhile, although the size of the engrafted HIOs was about 5 mm, fluorescent immunostaining revealed intestinal-specific markers only in small areas of the HIOs. Therefore, these results suggest that the remaining undifferentiated cells in the HIOs might have differentiated into other types of cells.

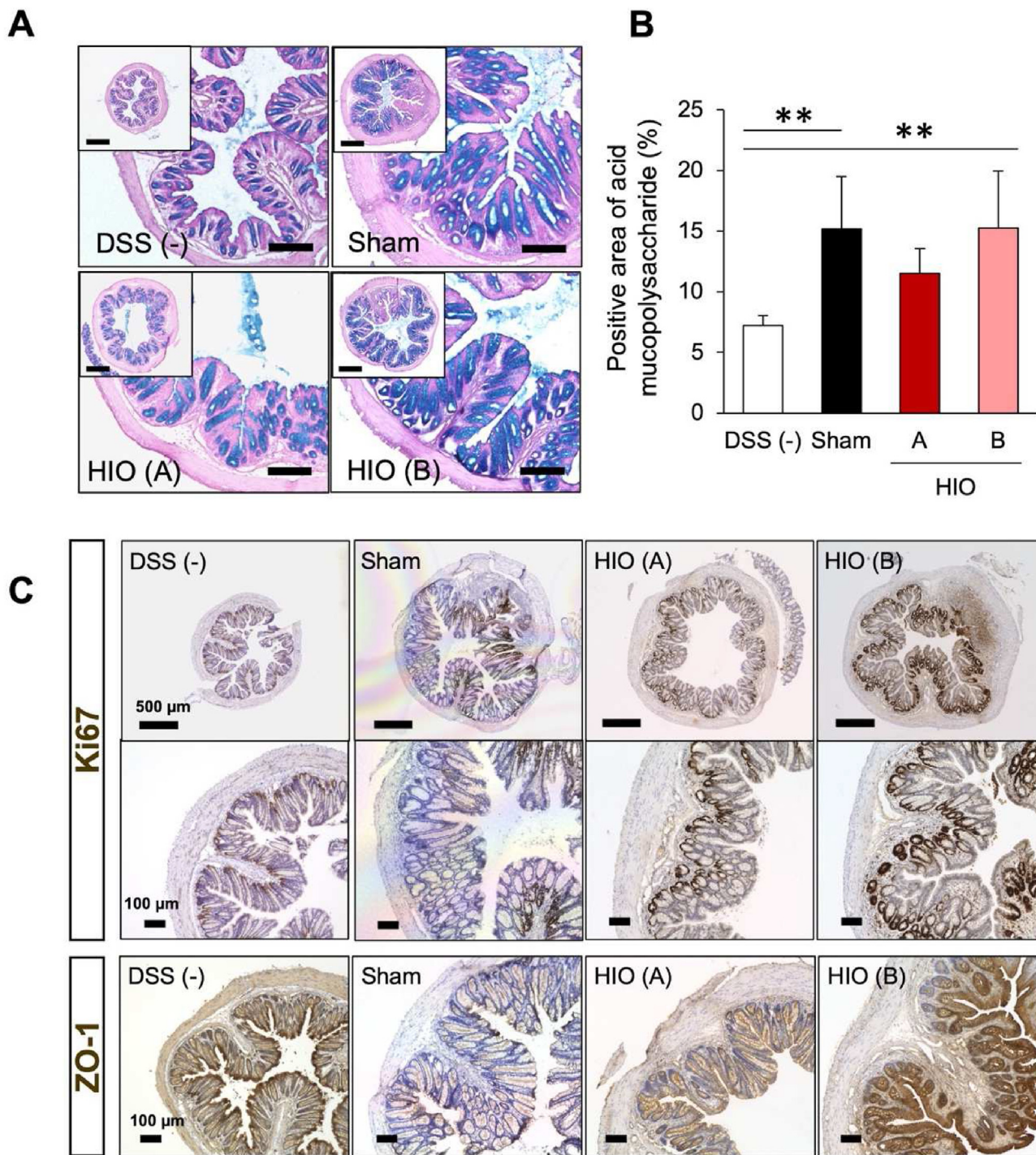


Fig. 4. Recovery of tissue damage via HIO injection. Nine days after injection, colon tissues were removed and stained (A) Alcian blue staining. The blue areas show acidic mucopolysaccharides, which is a component of mucus, and the pink area shows nuclei. Low magnitude images (upper left) for each group: scale bar = 500 μ m; high magnitude images: scale bar = 100 μ m (B) Quantification of acidic mucopolysaccharide. Positive area of acid mucopolysaccharide was calculated using the Hybrid Cell Count System. Data were shown as mean \pm SD ($n = 5$). $**p < 0.01$ (C) Immunohistochemical staining of Ki67 and ZO-1, a marker of tight junctions. Brown areas indicate positive areas for each antibody, while blue areas indicate nuclei. Scale bar = 500 μ m (upper), 100 μ m (middle and lower).

We then compared the clinical symptoms and colon tissues of acute colitis-model mice when injecting the two HIO types. Up to day 5 after injection, the HIO (A) group showed earlier improvement in body weight and clinical scores compared with the sham group, but on day 9 post injection, all groups recovered to the same level (Fig. 3B–D). This was an expected outcome as the colonic mucosa involved in water absorption also showed recovery to the

same level in all the groups. However, in patients who do not experience long-term remission, mucosal damage is often not completely repaired despite improvements in clinical symptoms [6,9]. Therefore, we analyzed mucus secretion and tight junctions, which are important in determining the state of intestinal mucosal injury. Goblet cells secrete mucus, which mainly consists of glycoproteins, to prevent intestinal flora from entering the body [34].

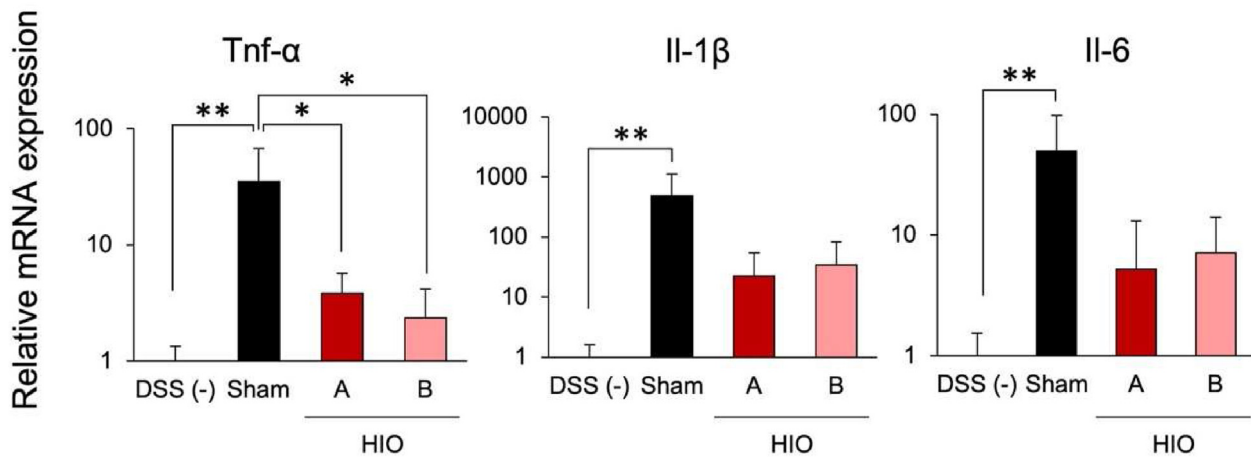


Fig. 5. Relative mRNA expression of proinflammatory cytokines in the colon 9 days after injection. The mRNA expression levels of DSS (-) were defined as 1. Data were shown as mean \pm SD ($n = 6$). * $p < 0.05$. ** $p < 0.01$.

One study reported that mucus secretion was increased by DSS-induced inflammation and returned to normal levels dependent on recovery [35]. Nine days after DSS discontinuation, the acid mucopolysaccharide level in the HIO (A) group was lower than that in the sham and HIO (B) groups and closer to that in the DSS (-) group (Fig. 4B). This indicates that the sham and HIO (B) groups recovered from inflammation more slowly than the HIO (A) group; the HIO (A) group progressed toward restoration a little earlier. In addition, the tight junctions between intestinal epithelial cells prevent the entry of xenobiotics. The loosening of these junctions is believed to be involved in disease progression [36,37]. After nine days of injection, ZO-1 expression in the sham group was lower than that in the other groups (Fig. 4C). Therefore, this suggested that the sham group had recovered enough function to gain weight; however, the tissue damage had not recovered sufficiently. We consider this to be a recurrence-prone condition, similar to that of patients with clinical UC. Remarkably, the HIO (A) group tended to have less colonic stricture than the sham and HIO (B) groups (Fig. 4C), indicating that the HIOs with higher intestinal stem cell expression contribute to the faster and more extensive restorative repair of mucosal damage than natural healing and may help prevent UC relapse (Fig. 4). The expression of Ki67 and ZO-1 was higher in the HIO (B) group than in the HIO (A) group. However, the higher expression of ZO-1 and Ki67 was related to slower repair in the HIO (B) group than in the HIO (A) group. Previous study has reported that intestinal stem cells transiently proliferate and mature into large number of epithelial cells in tissue repair, and then the inflammatory condition returns to normal [38]. That is, we considered that the state of HIO (B), which promotes the proliferation and barrier function, is pre-stage back to the state such as the HIO (A) group or DSS (-) group. These results were more pronounced in the colonic tissue, especially in the side closer to the anus. In this study, we considered that the effect of HIO was observed only in the vicinity of the HIO injection site; therefore, the analysis was limited to the colon tissue. However, the effects of HIO involving HIO contents and secretory factors could have been discussed further by analyzing other intestine tissue, such as the small intestine.

This study has several limitations. First, the HIOs could only be injected in mice during remission after the cessation of DSS administration. We could not examine the effect of HIO injection in the exacerbation phase with continued DSS administration because more than 50% of mice died during continuous DSS administration as a result of significant weight loss following injection. Second, we could not obtain data that supported the involvement of intestinal

stem cells and other component cells in HIOs during the repair of intestinal mucosal damage or data regarding the mechanism of tissue repair induced by the HIOs, especially by those having higher intestinal stem cell expression. We previously injected intestinal stem cells generated from human iPS cells into the colitis-model mice. However, it did not show tissue recovery as remarkable as was seen with the HIO injection (data not shown). Therefore, the presence of intestinal stem cells and the other cells surrounding the stem cells is important. To demonstrate that a specific cell population within the HIO is involved in the repair of intestinal mucosal damage, we require a technique to single-cell the HIO, select a specific cell population, and then transplant it. However, due to technical difficulties, further analysis was not possible. While the intestinal organoids have the advantage of containing multiple cells, they may have the disadvantage of being difficult to analyze for mechanisms. In addition, when HIOs were injected into the colitis-model mice, no human genes could be identified in the mouse colon. Therefore, unlike the results of transplantation studies on crypt-derived intestinal organoids reported previously, the HIOs generated by us did not directly repair mucosal tissues by engraftment. Nevertheless, the colon tissues after HIO (A) injections resembled those without DSS administration rather than those in the sham group (Fig. 4). The HIO injection groups also displayed lower mRNA expression levels of inflammatory cytokines compared with the sham group (Fig. 5). Additionally, the concentrated culture supernatants of HIO (A) tended to suppress weight loss better than the sham group as well as the injection of HIO (A) (Supplementary Fig. 2). These results suggest that HIO (A) might contain more factors that promote epithelial regeneration than HIO (B). Previous studies have reported that the conditioned medium and the extracts of intestinal epithelial cells and fibroblasts containing anti-inflammatory factors, especially prostaglandin E2, suppressed the production of proinflammatory cytokines by dendritic cells in the absence of functional regulatory T cells [39,40]. The HIOs used in the present study expressed villin-positive intestinal epithelial cells and vimentin-positive fibroblasts and were injected into immunodeficient mice lacking regulatory T cells. Therefore, we considered that prostaglandin E2 secreted from HIOs might have affected the dendritic cells and suppressed the production of inflammatory cytokines.

These findings suggest that HIOs do not directly repair intestinal mucosal damage by engraftment, but that the content or released factors of the HIOs, especially HIO (A), may be indirectly associated with the promotion of epithelial cell proliferation and inflammation

suppression. When iPS cell-derived cells are used for regenerative medicine, one issue is that residual undifferentiated cells may form tumors [41,42]. Therefore, in consideration of safety, showing effects that promote repair without engraftment may be convenient.

5. Conclusions

Effective cell therapy should directly repair tissue by engraftment at the site of injury. However, the difference in organoid property impacting the rate of tissue repair in transplantation without engraftment observed in the current study should be considered a critical consideration in the development of regenerative medicine using iPS-derived organoids.

Ethics approval and consent to participate

All animal experiments were approved by the Institutional Laboratory Animal Care and Use Committee of Nagoya City University (Idou 20-013R21).

Consent for publication

Not applicable.

Availability of data and materials

Not applicable (Data generated or analyzed during this study are included in this published article and its supplementary information files.)

Authors' contributions

AN, ST, DO, TH, and TM conceived and presented the idea. AN and DO designed and conducted the differentiation induction experiments. AN, ST, and CW designed and performed the animal experiments. AN and CW analyzed the data. AN, ST, DO, CW, TH, TI, and TM interpreted the results. AN contributed significantly to the drafting of the manuscript. TH, TI, and TM reviewed and edited the manuscript. The authors read and approved the final manuscript.

Declaration of competing interest

The authors declare no conflicts of interest.

Acknowledgments

We thank Dr. Hidenori Akutsu, Dr. Yoshitaka Miyagawa, Dr. Hajime Okita, Dr. Nobutaka Kiyokawa, Dr. Masashi Toyoda, and Dr. Akihiro Umezawa for providing human iPS cells. This work was supported by a grant-in-aid from the Japan Agency for Medical Research and Development (AMED), grant number JP20be0304203. We also thank Enago (www.enago.jp) for the English language review.

Appendix A. Supplementary data

Supplementary data to this article can be found online at <https://doi.org/10.1016/j.reth.2022.08.004>.

References

- [1] Atreya R, Neurath MF, Siegmund B. Personalizing Treatment in IBD: hype or reality in 2020? Can we predict response to anti-TNF? *Front Med* 2020;7:517.
- [2] van Dullemen HM, van Deventer SJ, Hommes DW, Bijl HA, Jansen J, Tytgat GN, et al. Treatment of Crohn's disease with anti-tumor necrosis factor chimeric monoclonal antibody (cA2). *Gastroenterology* 1995;109:129–35.
- [3] Ford AC, Sandborn WJ, Khan KJ, Hanauer SB, Talley NJ, Moayyedi P. Efficacy of biological therapies in inflammatory bowel disease: systematic review and meta-analysis. *Am J Gastroenterol* 2011;106:644–59. quiz 60.
- [4] Okamoto R, Shimizu H, Suzuki K, Kawamoto A, Takahashi J, Kawai M, et al. Organoid-based regenerative medicine for inflammatory bowel disease. *Regen Ther* 2020;13:1–6.
- [5] Lichtenstein GR, Rutgeerts P. Importance of mucosal healing in ulcerative colitis. *Inflamm Bowel Dis* 2010;16:338–46.
- [6] Frosli KE, Jahnsen J, Moum BA, Vatn MH, Group I. Mucosal healing in inflammatory bowel disease: results from a Norwegian population-based cohort. *Gastroenterology* 2007;133:412–22.
- [7] Kim DH, Cheon JH. Pathogenesis of inflammatory bowel disease and recent advances in biologic therapies. *Immune Netw* 2017;17:25–40.
- [8] Shimizu H, Suzuki K, Watanabe M, Okamoto R. Stem cell-based therapy for inflammatory bowel disease. *Int Res* 2019;17:311–6.
- [9] Neurath MF, Travis SP. Mucosal healing in inflammatory bowel diseases: a systematic review. *Gut* 2012;61:1619–35.
- [10] Wang Y, Chen X, Cao W, Shi Y. Plasticity of mesenchymal stem cells in immunomodulation: pathological and therapeutic implications. *Nat Immunol* 2014;15:1009–16.
- [11] Soontararak S, Chow L, Johnson V, Coy J, Wheat W, Regan D, et al. Mesenchymal stem cells (MSC) derived from induced pluripotent stem cells (iPSC) equivalent to adipose-derived MSC in promoting intestinal healing and microbiome normalization in mouse inflammatory bowel disease model. *Stem Cells Transl Med* 2018;7:456–67.
- [12] Holmberg FE, Seidelin JB, Yin X, Mead BE, Tong Z, Li Y, et al. Culturing human intestinal stem cells for regenerative applications in the treatment of inflammatory bowel disease. *EMBO Mol Med* 2017;9:558–70.
- [13] Sugimoto S, Ohta Y, Fujii M, Matano M, Shimokawa M, Nanki K, et al. Reconstruction of the human colon epithelium in vivo. *Cell Stem Cell* 2018;22:171–176 e5.
- [14] Sato T, Stange DE, Ferrante M, Vries RG, Van Es JH, Van den Brink S, et al. Long-term expansion of epithelial organoids from human colon, adenoma, adenocarcinoma, and Barrett's epithelium. *Gastroenterology* 2011;141:1762–72.
- [15] Fujii M, Matano M, Toshimitsu K, Takano A, Mikami Y, Nishikori S, et al. Human intestinal organoids maintain self-renewal capacity and cellular diversity in niche-inspired culture condition. *Cell Stem Cell* 2018;23:787–793 e6.
- [16] Seki T, Yuasa S, Fukuda K. Generation of induced pluripotent stem cells from a small amount of human peripheral blood using a combination of activated T cells and Sendai virus. *Nat Protoc* 2012;7:718–28.
- [17] Umekage M, Sato Y, Takasu N. Overview: an iPS cell stock at CiRA. *Inflamm Regen* 2019;39:17.
- [18] de Rham C, Villard J. Potential and limitation of HLA-based banking of human pluripotent stem cells for cell therapy. *J Immunol* 2014;2014:518135.
- [19] Morishima Y, Azuma F, Kashiwase K, Matsumoto K, Orihara T, Yabe H, et al. Risk of HLA homozygous cord blood transplantation: implications for induced pluripotent stem cell banking and transplantation. *Stem Cells Transl Med* 2018;7:173–9.
- [20] McCracken KW, Howell JC, Wells JM, Spence JR. Generating human intestinal tissue from pluripotent stem cells in vitro. *Nat Protoc* 2011;6:1920–8.
- [21] Spence JR, Mayhew CN, Rankin SA, Kuhar MF, Vallance JE, Tolle K, et al. Directed differentiation of human pluripotent stem cells into intestinal tissue in vitro. *Nature* 2011;470:105–9.
- [22] Yoshida S, Miwa H, Kawachi T, Kume S, Takahashi K. Generation of intestinal organoids derived from human pluripotent stem cells for drug testing. *Sci Rep* 2020;10:5989.
- [23] https://web.expasy.org/cellosaurus/CVCL_0440.
- [24] Onozato D, Yamashita M, Nakanishi A, Akagawa T, Kida Y, Ogawa I, et al. Generation of intestinal organoids suitable for pharmacokinetic studies from human induced pluripotent stem cells. *Drug Metab Dispos* 2018;46:1572–80.
- [25] Watson CL, Mahe MM, Munera J, Howell JC, Sundaram N, Poling HM, et al. An in vivo model of human small intestine using pluripotent stem cells. *Nat Med* 2014;20:1310–4.
- [26] Finkbeiner SR, Hill DR, Altheim CH, Dedhia PH, Taylor MJ, Tsai YH, et al. Transcriptome-wide analysis reveals hallmarks of human intestine development and maturation in vitro and in vivo. *Stem Cell Rep* 2015;4:1140–55.
- [27] Chassaing B, Aitken JD, Malleshappa M, Vijay-Kumar M. Dextran sulfate sodium (DSS)-induced colitis in mice. *Curr Protoc Im* 2014;104. 15 25 1–15 25 14.
- [28] Park JS, Yi TG, Park JM, Han YM, Kim JH, Shin DH, et al. Therapeutic effects of mouse bone marrow-derived clonal mesenchymal stem cells in a mouse model of inflammatory bowel disease. *J Clin Biochem Nutr* 2015;57:192–203.
- [29] Wirtz S, Neufert C, Weigmann B, Neurath MF. Chemically induced mouse models of intestinal inflammation. *Nat Protoc* 2007;2:541–6.
- [30] Cruz-Acuna R, Quiros M, Farkas AE, Dedhia PH, Huang S, Siuda D, et al. Synthetic hydrogels for human intestinal organoid generation and colonic wound repair. *Nat Cell Biol* 2017;19:1326–35.
- [31] Yui S, Nakamura T, Sato T, Nemoto Y, Mizutani T, Zheng X, et al. Functional engraftment of colon epithelium expanded in vitro from a single adult Lgr5(+) stem cell. *Nat Med* 2012;18:618–23.
- [32] Tsai YH, Nattiv R, Dedhia PH, Nagy MS, Chin AM, Thomson M, et al. In vitro patterning of pluripotent stem cell-derived intestine recapitulates in vivo human development. *Development* 2017;144:1045–55.

- [33] Zhu F, Sun B, Wen Y, Wang Z, Reijo Pera R, Chen B. A modified method for implantation of pluripotent stem cells under the rodent kidney capsule. *Stem Cell Dev* 2014;23:2119–25.
- [34] Johansson ME, Hansson GC. Mucus and the goblet cell. *Dig Dis* 2013;31:305–9.
- [35] Kimura I, Kamiya A, Nagahama S, Yoshida J, Tanigawa H, Kataoka M. Study on the experimental ulcerative colitis model induced by dextran sulfate sodium in rats: estimation of mucosal erosions by the alcian blue-staining method. *Nihon Yakurigaku Zasshi* 1993;102:343–50.
- [36] Landy J, Ronde E, English N, Clark SK, Hart AL, Knight SC, et al. Tight junctions in inflammatory bowel diseases and inflammatory bowel disease associated colorectal cancer. *World J Gastroenterol* 2016;22:3117–26.
- [37] Yang M, Jia W, Wang D, Han F, Niu W, Zhang H, et al. Effects and mechanism of constitutive TL1A expression on intestinal mucosal barrier in DSS-induced colitis. *Dig Dis Sci* 2019;64:1844–56.
- [38] Barker N. Adult intestinal stem cells: critical drivers of epithelial homeostasis and regeneration. *Nat Rev Mol Cell Biol* 2014;15(1):19–33.
- [39] Chinen T, Komai K, Muto G, Morita R, Inoue N, Yoshida H, et al. Prostaglandin e2 and socs1 have a role in intestinal immune tolerance. *Nat Commun* 2011;2:190.
- [40] Shiraishi H, Yoshida H, Saeki K, Miura Y, Watanabe S, Ishizaki T, et al. Prostaglandin e2 is a major soluble factor produced by stromal cells for preventing inflammatory cytokine production from dendritic cells. *Int Immunol* 2008;20(9):1219–29.
- [41] Miura K, Okada Y, Aoi T, Okada A, Takahashi K, Okita K, et al. Variation in the safety of induced pluripotent stem cell lines. *Nat Biotechnol* 2009;27:743–5.
- [42] Nishimori M, Yakushiji H, Mori M, Miyamoto T, Yaguchi T, Ohno S, et al. Tumorigenesis in cells derived from induced pluripotent stem cells. *Hum Cell* 2014;27:29–35.